BULLETIN OF THE POLISH ACADEMY OF SCIENCES
TECHNICAL SCIENCES, Vol. 62, No. 2, 2014
*DOI: 10.2478/bpasts-2014-0028*

Dedicated to Professor J. Klamka
on the occasion of his 70th birthday

# Stability analysis of hybrid active power filter

D. BUŁA* and M. PASKO

Institute of Electrotechnics and Computer Science, Silesian University of Technology, 10 Akademicka St., 44-100 Gliwice, Poland

**Abstract.** In the paper the analysis of a three-phase hybrid active power filter stability has been presented. Configuration with a single tuned passive filter was used as an example. However, the analysis can be applied to similar configurations of hybrid filters with closed loop control.

The article presents a model of the analyzed system in the frequency domain. The division of the model into two independent systems, for positive and negative components, allowed to apply the Nyquist criterion for the stability analysis in this case. As a part of the analysis, the effect of delays, control signal filter parameters, and passive filter parameters have been examined. Based on the presented stability analysis, system parameters for the experimental model of a hybrid power filter have been selected. Finally, experimental results confirming the validity of the analysis have been shown.

**Key words:** active power filter, hybrid filters, power quality, higher harmonics, stability analysis.

## 1. Introduction

Harmonics generated by nonlinear loads are one of significant problems of power quality. The most commonly used solution to harmonics problem is applying passive filters. The main disadvantage of this method is that filtering characteristic depends on source impedance, which is usually variable. Moreover, resonance between the passive filter and source impedance may occur [1]. Another solution, deprived of the mentioned drawbacks, is making use of active power filters (APF) [2–6]. Nevertheless, it can be too expensive in case of high power systems. Therefore, in this case hybrid active power filters (HAPF) could be an alternative. HAPF are a combination of active power filters and passive filters [2, 3, 7–18]. By employing a combination of both solutions, much better filtration properties and lower sensitivity to main system parameters, compared to passive filters, are obtained. This also enables to reduce the required power, voltage or currents of an active power filter, which in turn allows it to be used for example in medium voltage networks. Two configurations have been mainly used: a series active filter combined with a shunt passive filter [8, 14, 16, 17] and a shunt active filter connected in series with a shunt passive filter [7, 9–13, 16, 18].

In this paper the second kind of topology has been considered. The concept of system configuration has been presented in Fig. 1. In this case, on the terminals of the APF full mains voltage does not appear which allows to significantly reduce the $u_{dc}$ voltage and the cost of the whole filter. The control is usually performed in a closed loop system by generating an APF voltage output proportional to the higher harmonics of source currents [2, 3, 7, 9]:

$$v_F = K i_{S(hh)}, \tag{1}$$

where $K$ – gain of hybrid filter, $i_{S(hh)}$ – higher harmonics of source currents.

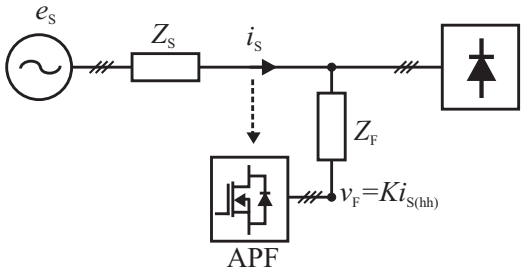


Fig. 1. Hybrid active power filter - serial connection of parallel active power filter (APF) with a passive filter

Working in a closed system may cause stability problems which necessitates the need to reduce $K$ gain. An additional problem is the delay occurring in the control system, which has a significant impact on the stability of the system. Therefore a stability analysis at the design stage of the HAPF is necessary. In this analysis the following elements should be taken into account:

- the control method and its parameters, such as signal filter parameters,
- passive filter elements,
- the power line parameters,
- the time delay in the processing circuit.

The stability problem of systems with active power filters and hybrid filters has been discussed in several papers [2, 4–8, 13–19]. Authors usually examine the stability of the system for the specific case by evaluating the phase margin. In these papers, the significant impact of delays in the control on the

*e-mail: dawid.bula@polsl.pl

stability of the system has been noticed. However, a simplified single-phase model of the analyzed system has been used, which may not give accurate results. Only in the article [14] the full three-phase model was used, but the analysis concerned a series configuration of a hybrid filter, and did not include delays in the system.

In the work [15] the impact of passive filter parameters on the stability of the system has also been highlighted. The authors showed Nyquist plots for different values of passive filter parameters. Additionally, in articles concerning the hybrid filters [16–18] and the active power filters [19], the possibility of modifying the control system to reduce or eliminate the impact of the delay on the system stability has been shown.

This article concerns the hybrid power filter in configuration with a single tuned passive filter. The control system of the considered hybrid filter allows it to work properly with balanced as well as unbalanced load. In this paper, a full three-phase model in frequency domain has been used. The used model, after separating positive and negative components, allowed to apply the Nyquist criterion for the stability analysis. Based on the presented analysis, the dependence of the critical gain of the hybrid power filter on the delay in the system as well as passive filter parameters (capacitance) has been shown. Additionally, the effect of the order of the signal filters used in the control circuit on the system stability has been presented. The analysis allowed the optimal selection of hybrid power filter parameters, which was confirmed by the experimental results.

## 2. The considered HAPF

A scheme of the considered hybrid active power filter has been shown in Fig. 2. Unlike the most commonly applied systems, the HAPF contains a passive filter tuned to one harmonic ($7^{th}$). This allows to reduce the size and cost of the whole filter, but requires the modification of the control algorithm. In this case, it consists in the generation of additional output voltage dependent on specific harmonic of load currents [5, 11, 13]. It enables to influence filter characteristics for selected harmonics. The consequence of the dependence on load current ($i_{\mathrm{L}}$) is the fact that this part of control works in an open loop system and has no effect on the stability. For this reason, in the further analysis, parts specific for HAPF with a single tuned passive filter were omitted. The part responsible for controlling the $u_{\mathrm{dc}}$ voltage was also omitted, as this is a subordinate control system without a significant impact on the stability of the whole system. The influence of the voltage inverter was likewise not taken into account. Without these assumptions general term stability of the system can be very complex [20].

To determine the higher harmonics of source current, a method based on Park transform [2, 7, 10] has been used. The block diagram of the control algorithm shown in Fig. 3 can be divided into two branches: the lower – responsible for filtering fundamental harmonic positive sequence component ($\omega_1$) and the upper – responsible for filtering fundamental harmonic negative sequence component ($-\omega_1$). In the end, the harmonics of source currents in the general case of an unbalanced load have been achieved:

$$i_{\mathrm{S1,2,3(hh)}} = \sqrt{2}\mathrm{Re}\sum_{h\in\mathrm{N},h>1} I_{\mathrm{S1,2,3(h)}}\mathrm{e}^{\mathrm{j}h\omega_1 t}. \tag{2}$$

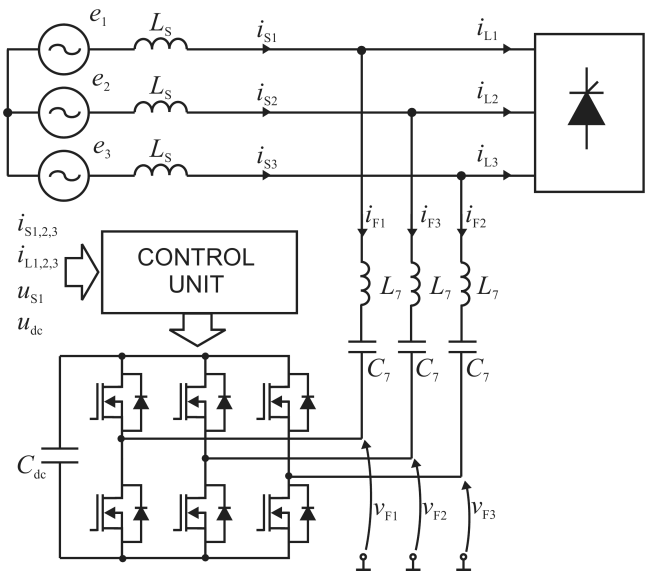


Fig. 2. Three phase hybrid power filter with a single tuned passive filter

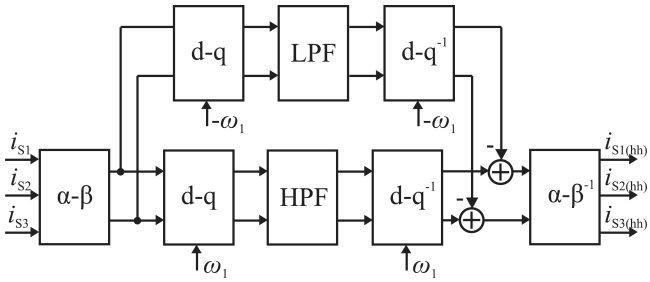


Fig. 3. The control algorithm responsible for obtaining the higher harmonics of source currents

For the presented system and the control algorithm a derivation of the model in the frequency domain for the $\alpha-\beta$ coordinates is possible. The diagram of the model is shown in Fig. 4. The block $G_1(\mathrm{j}\omega)$ applied in the model represents the matrix associated with Park transformation and signal filters (LPF, HPF), which can be written as [10]:

$$\mathbf{G}_1(\mathrm{j}\omega) = \mathbf{G}'(\mathrm{j}\omega) - \mathbf{G}''(\mathrm{j}\omega), \tag{3}$$

$\mathbf{G}'(\mathrm{j}\omega)$ – matrix associated with Park transformation and HPF filters for positive sequence of fundamental frequency:

$$\mathbf{G}'(\mathrm{j}\omega) = \mathbf{D}^{-1}_{\mathrm{HPF}}(\lambda')\mathbf{N}_{\mathrm{HPF}}(\lambda'), \tag{4}$$

$$\lambda' = \begin{bmatrix} \mathrm{j}\omega & \omega_0 \\ -\omega_0 & \mathrm{j}\omega \end{bmatrix}, \tag{5}$$

$$K_{\mathrm{HPF}}(\mathrm{j}\omega) = \frac{N_{\mathrm{HPF}}(\mathrm{j}\omega)}{D_{\mathrm{HPF}}(\mathrm{j}\omega)}, \tag{6}$$

$\mathbf{G}''(\mathrm{j}\omega)$ – matrix associated with Park transformation and LPF filters for negative sequence of fundamental frequency:

$$\mathbf{G}''(\mathrm{j}\omega) = \mathbf{D}_{\mathrm{LPF}}^{-1}(\lambda'')\mathbf{N}_{\mathrm{LPF}}(\lambda''), \tag{7}$$

$$\lambda'' = \begin{bmatrix} \mathrm{j}\omega & -\omega_0 \\ \omega_0 & \mathrm{j}\omega \end{bmatrix}, \tag{8}$$

$$K_{\mathrm{LPF}}(\mathrm{j}\omega) = \frac{N_{\mathrm{LPF}}(\mathrm{j}\omega)}{D_{\mathrm{LPF}}(\mathrm{j}\omega)}. \tag{9}$$

For the presented model, the relationship binding source currents and load currents in $\alpha - \beta$ coordinates can be the following:

$$\begin{bmatrix} I_{\mathrm{S}\alpha}(\mathrm{j}\omega) \\ I_{\mathrm{S}\beta}(\mathrm{j}\omega) \end{bmatrix} = \mathbf{G}(\mathrm{j}\omega) \begin{bmatrix} I_{\mathrm{L}\alpha}(\mathrm{j}\omega) \\ I_{\mathrm{L}\beta}(\mathrm{j}\omega) \end{bmatrix}, \tag{10}$$

$$\mathbf{G}(\mathrm{j}\omega) = \left[Z_{\mathrm{F}}(\mathrm{j}\omega)\mathbf{1}_2 + Z_{\mathrm{S}}(\mathrm{j}\omega)\mathbf{1}_2 + K\mathbf{G}_1(\mathrm{j}\omega)\right]^{-1} Z_{\mathrm{F}}(\mathrm{j}\omega), \tag{11}$$

where $\mathbf{1}_2$ – $2 \times 2$ unit matrix, $Z_F(\mathrm{j}\omega)$ – passive filter impedance, $Z_S(\mathrm{j}\omega)$ – source/line impedance, $K$ – hybrid filter gain.

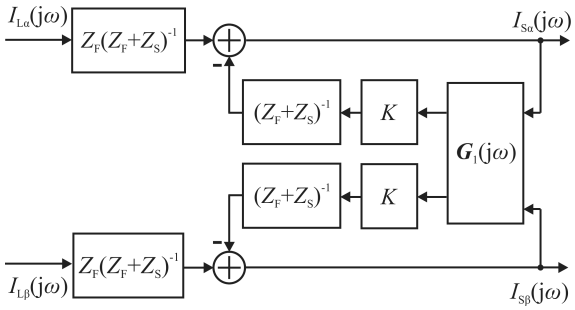


Fig. 4. Frequency model of hybrid active power filter

## 3. Stability analysis

The stability analysis of the system shown in Fig. 4 could be troublesome. Therefore the model has been transformed from $\alpha - \beta$ coordinates into two independent systems for positive and negative sequences. This transformation was carried out according to the following relationships:
based on:

$$\begin{bmatrix} I^+ \\ I^- \end{bmatrix} = \mathbf{C} \begin{bmatrix} I_\alpha \\ I_\beta \end{bmatrix} = \sqrt{\frac{1}{2}} \begin{bmatrix} 1 & \mathrm{j} \\ 1 & -\mathrm{j} \end{bmatrix} \begin{bmatrix} I_\alpha \\ I_\beta \end{bmatrix}, \tag{12}$$

(10) can be can be expressed by:

$$\begin{bmatrix} I_{\mathrm{S}}^+(\mathrm{j}\omega) \\ I_{\mathrm{S}}^-(\mathrm{j}\omega) \end{bmatrix} = \mathbf{G}^{+,-}(\mathrm{j}\omega) \begin{bmatrix} I_{\mathrm{L}}^+(\mathrm{j}\omega) \\ I_{\mathrm{L}}^-(\mathrm{j}\omega) \end{bmatrix}, \tag{13}$$

$$\mathbf{G}^{+,-}(\mathrm{j}\omega) = \left[Z_{\mathrm{F}}(\mathrm{j}\omega)\mathbf{1}_2 + Z_{\mathrm{s}}(\mathrm{j}\omega)\mathbf{1}_2 + K\mathbf{G}_1^{+,-}(\mathrm{j}\omega)\right]^{-1} Z_{\mathrm{F}}(\mathrm{j}\omega), \tag{14}$$

where

$$\mathbf{G}_1^{+,-}(\mathrm{j}\omega) = \mathbf{C}\mathbf{G}_1(\mathrm{j}\omega)\mathbf{C}^{-1} \tag{15}$$

and

$$\mathbf{G}_1^{+,-}(\mathrm{j}\omega) = \begin{bmatrix} G_1^+(\mathrm{j}\omega) & 0 \\ 0 & G_1^-(\mathrm{j}\omega) \end{bmatrix}. \tag{16}$$

As a result of the transformation to positive and negative sequences a model shown in Fig. 5 has been obtained. It can be used for further stability analysis.

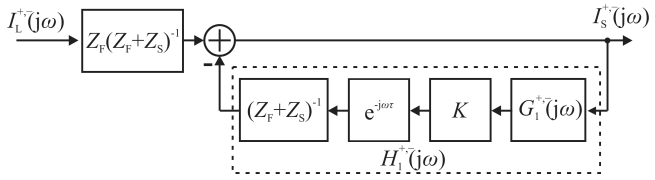


Fig. 5. Frequency model used in the stability analysis

The additional delay ($\tau$) in the feedback was also entered there. The delay represents the real delays in control processing [2, 10, 13, 17, 21]. The model is independent for positive (+) and negative components (−), so it can be analyzed as a simple model with feedback and delay. Feedback transfer functions are the following:

$$H_1^{+,-}(\mathrm{j}\omega) = \frac{KG_1^{+,-}(\mathrm{j}\omega)\mathrm{e}^{-\mathrm{j}\omega\tau}}{Z_{\mathrm{F}}(\mathrm{j}\omega) + Z_{\mathrm{S}}(\mathrm{j}\omega)}. \tag{17}$$

a)

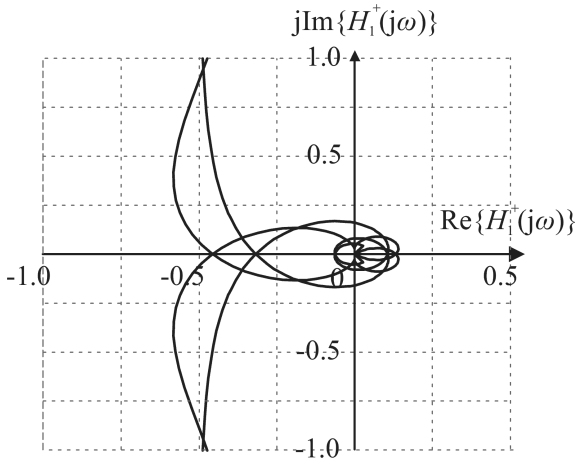


b)

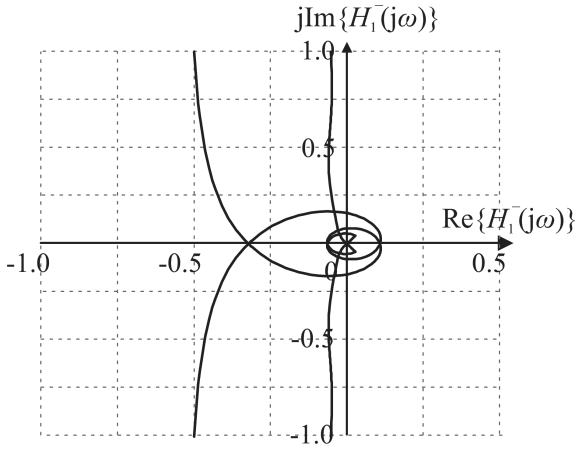


Fig. 6. Nyquist plots for transfer functions: a) $H_1^+(\mathrm{j}\omega)$ and b) $H_1^-(\mathrm{j}\omega)$

On this basis it is possible to check the stability according to Nyquist criterion. Exemplary Nyquist plots for transfer functions $H_1^+(\mathrm{j}\omega)$ and $H_1^-(\mathrm{j}\omega)$ have been shown in Fig. 6. The parameters used for the analysis are shown in Table 1. It can be seen that in this case the system is stable and filter parameters are properly matched.

Table 1
System parameters

| | |
|---|---|
| Filter gain | $K = 25$ |
| LPF filter | 2nd order Butterworth $f_c = 25$ Hz |
| HPF filter | 2nd order Butterworth $f_c = 25$ Hz |
| Delay | $\tau = 100$ $\mu$s |
| Source | $\lvert E_{1,2,3}\rvert = 230$ V, $R_S = 0.1$ Ω, $L_S = 0.2$ mH |
| Passive filter | $L_7 = 4.2$ mH, $C_7 = 50$ $\mu$F, $R_7 = 0.4$ Ω |

## 4. Influence of signal filters on stability

Depending on the choice of the type and parameters of signal filters in the control algorithm, it is possible to form characteristics of the filter circuit. They have an influence on the dynamic properties of the system [10]. Because their parameters occur in the feedback loop, they also influence stability. Providing the first-order filters are used without delays in the processing circuit, the system is always stable. With the increase in the delay time of such a system, critical gain decreases. In case of a higher-order signal filter, the system can be unstable even without delay. An example of graph $K_{\text{crit.}} = f(\tau)$ for the 1st order filter with 16 Hz cut-off frequency and the 2nd order Butterworth filter with 25 Hz cut-off frequency is shown in Fig. 7.

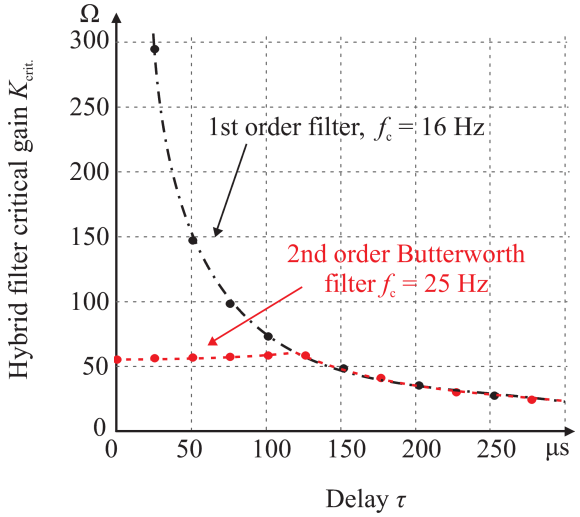


Fig. 7. Graph of critical HAPF gain $K_{\text{crit.}} = f(\tau)$ for 1st and 2nd order filters

## 5. Influence of passive filter parameters on stability

A hybrid power filter in the considered configuration works also as a static reactive power compensator. Therefore, passive filter parameters usually depend on the assumed reactive power for a fundamental harmonic. In addition, the capacitance value of the filter influences the value of active part currents. However, at the design stage it is possible to choose passive filter parameters i.e. inductance and capacitance of filter. These parameters highly influence the stability of the hybrid power filter. For example, in Fig. 8, the graph presenting the dependence between the critical gain $K_{\text{crit.}}$ and the passive filter capacity has been shown. The inverse proportionality in this case is clearly seen. From the point of view of the stability of the analyzed HAPF, capacitors with lower capacity in passive filters should be used.

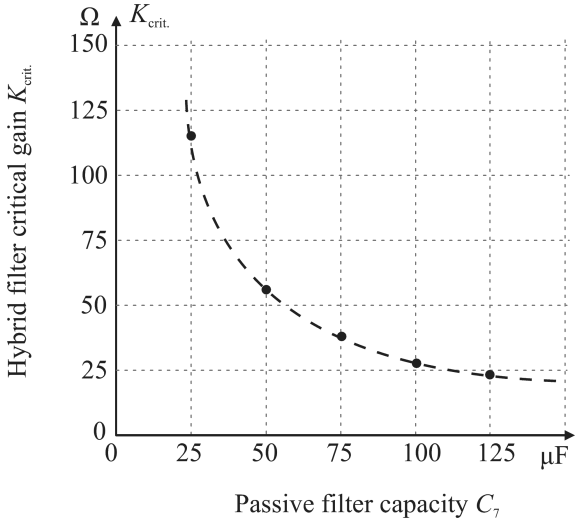


Fig. 8. Graph of critical HAPF gain $K_{\text{crit.}} = f(C_7)$, $\tau = 100$ $\mu$s, $Q_7 = 18$, $C_7 L_7$ = const

Additionally, in Fig. 9 the relationship $K_{\text{crit.}} = f(\tau, C_7)$ in 3D graph has been presented. Using this relationship it is possible to evaluate the stability for the specific capacitance value of the passive filter and the delay in the control circuit. On the basis of the presented graph it can be further noted that for the analyzed case, regardless of the value of the capacitor, there is a delay value above which the critical gain drops sharply. Here this particular delay value is about 120 $\mu$s.

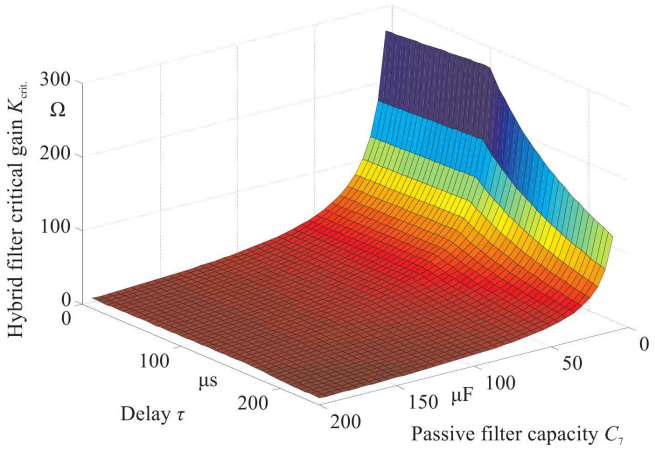


Fig. 9. Graph of critical HAPF gain $K_{\text{crit.}} = f(\tau, C_7)$, $Q_7 = 18$, $C_7 L_7$ = const

## 6. Simulation results

The primary objective of the simulation results presentation concerning the analyzed system was to show that for large delay values the system becomes unstable. The hybrid active power filter shown in Fig. 2 has been simulated with parameters from Table 1. The 5 kW diode rectifier has been used as load. The simulation has been carried out for two different delays in the control circuit: 100 $\mu$s and 400 $\mu$s. The results of the simulation have been presented in Fig. 10. It can be seen that in case of 400 $\mu$s delay, the system is unstable, which confirms the results of the prior analysis (Fig 7).

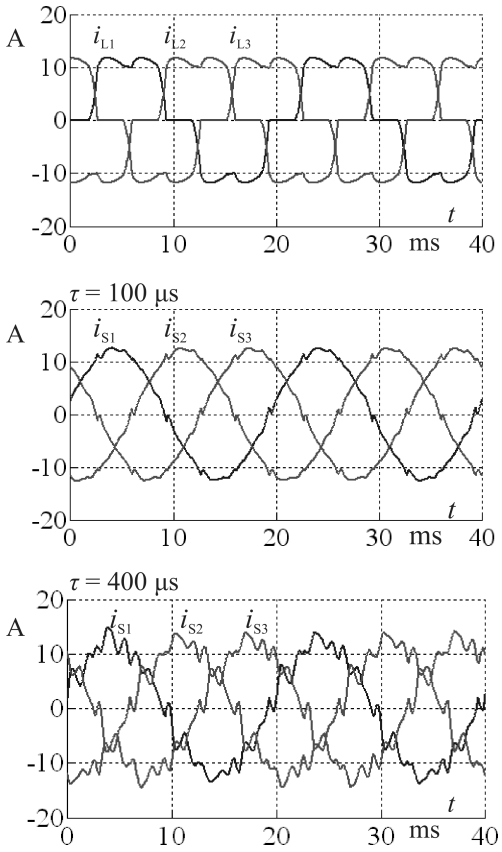


Fig. 10. Simulation results for different delay time

The second set of simulation results is shown for the comparison of the dynamics of a hybrid filter for different signal filters. As shown in the relationship in Fig. 7, for small values of delay, the 1st order filter provides greater value of critical gain. However, the selection of the filter has an impact on the dynamics of the system, as it was described in [10]. The Fig. 11 shows the transient state comparison using two different signal filters in the control system. The transient state was obtained by changing the load power. In the first case, the 2nd order Butterworth filter with a 2 Hz cutoff frequency was used. The second case was obtained by using 1st order filters with 12 Hz cutoff frequency. Cutoff frequencies are chosen so as to provide the same quality of HAPF filtration in a steady-state. In the case of 1st order filters, the response time of the signal filters causes a longer transient state in line currents when load power changing. Therefore, although the 1st order signal filters provide greater stability margin, 2nd order filters were used in the experimental model.

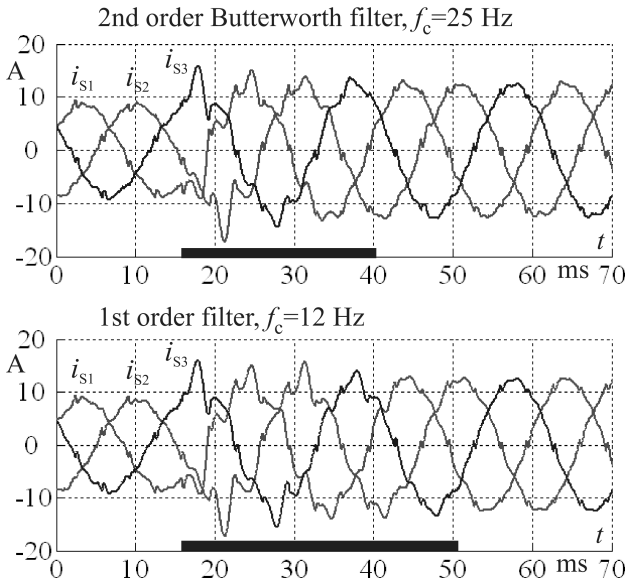


Fig. 11. Simulation results – transient state for different signal filters

## 7. Experimental results

Pictures of the laboratory model which was used in the experimental tests have been presented in Fig. 12. The model is composed of:

- passive part with 7th harmonic filters,
- Voltage Source Inverter (VSI) with IRFP250NPbF transistors,
- control unit with TMS320F28335 floating-point digital signal controller,
- measuring system consisting of LEM current transducers.

Experimental tests for the discussed hybrid power filter have been made with the parameters presented in Table 2.

Table 2
System parameters for experimental results

| | |
|---|---|
| Filter gain | $K = 25$ |
| Source | $\|E_{1,2,3}\| = 230$ V, $L_S = 0.3$ mH |
| Passive filter | $L_7 = 4.2$ mH, $C_7 = 50$ $\mu$F, $R_7 = 0.4$ $\Omega$ |
| DC Link | $U_{dc(ref)} = 60$ V, $C_{dc} = 4700$ $\mu$F |
| VSI | $f_{PWM} = 25$ kHz, $t_d = 0.8$ $\mu$s |
| Load 1 | Balanced 3.5–5 kW diode rectifier |
| Load 2 | Load 1 + 2 kW unbalanced linear load |

Selection of the HAPF parameters was based, inter alia, on the analysis of stability:

- Signal filters – a 2nd order signal filter has been chosen due to the dynamics of the system (Fig. 11);
- Passive filter – passive filter $C_7$ capacity with a relatively small value (50 $\mu$F) was used. Even a smaller value would require to increase the inductance $L_7$ value and therefore to increase the device dimensions and the passive filter quality deterioration;

- Delay – 40 $\mu$s resulted directly from the operating frequency. At that time, the required measurements of signals are made, all calculations are carried out and transistors gate signals are set;
- Filter gain – for such selected parameters, critical gain is equal 53. However, to provide a wide margin of stability, gain was set to 25. It is sufficient to obtain the required quality of harmonic filtration, which is confirmed by the experimental results.

Phase margin for such selected parameters is 77°.

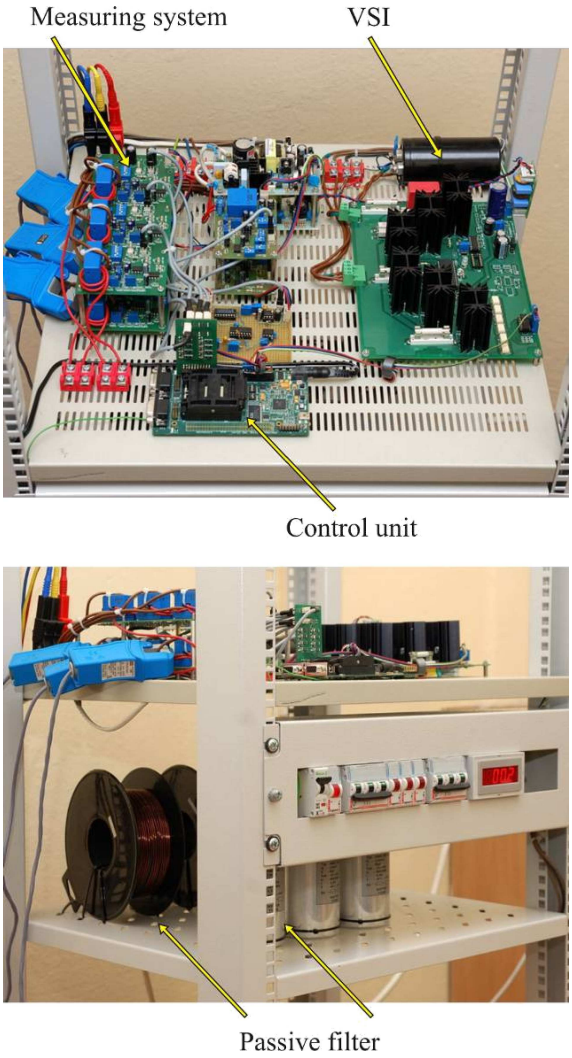


Fig. 12. Laboratory model of the hybrid power filter

Two load cases have been used in the experimental tests. The first test was made for the balanced nonlinear load and consisted in the gradual changing of the load – from 3.5 kW to 5 kW. The second one consisted in connecting 2 kW unbalanced linear load to a 3.5 kW balanced nonlinear load. Changes of the load were intended to verify whether the system becomes unstable or not. The experimental results have been presented in Fig. 14 and Fig. 16 whereas the results for steady states after load change have been shown in Fig. 13 and Fig. 15. Total harmonic distortions (THD) of source currents after load change have been shown in Table 3.

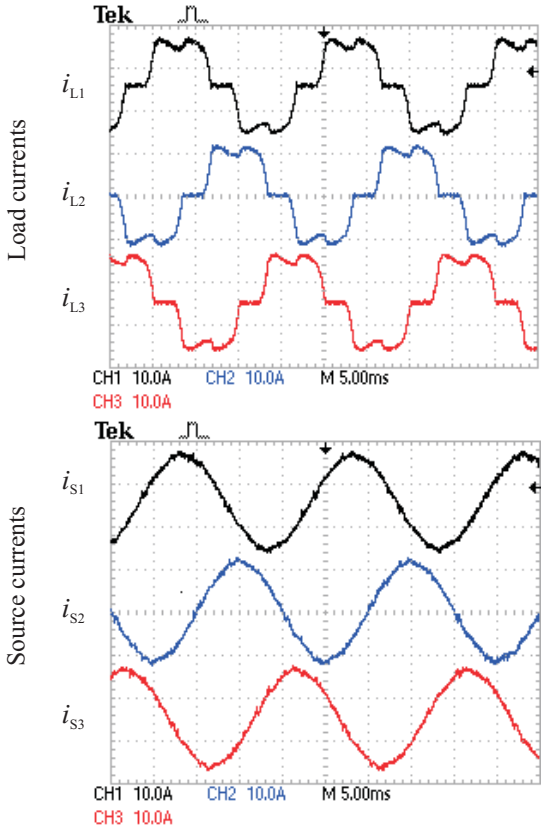


Fig. 13. Experimental results for a balanced load – steady state

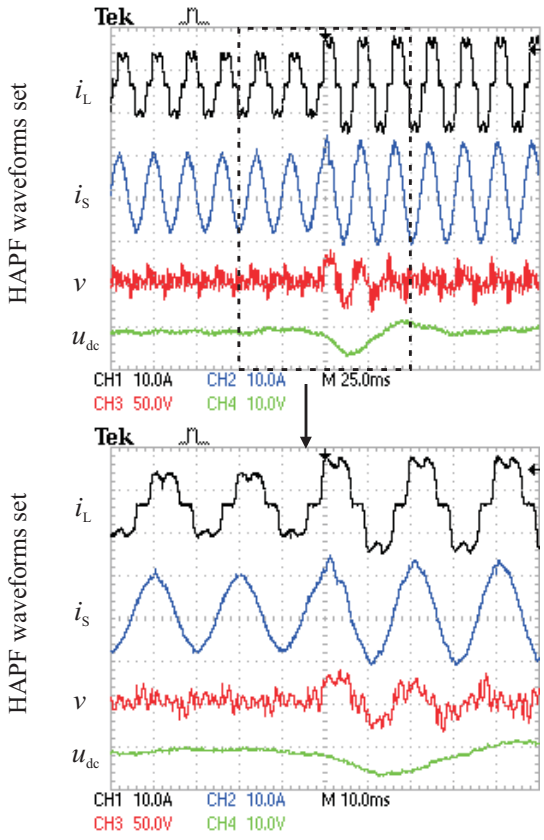


Fig. 14. Experimental results for a balanced load – transient state

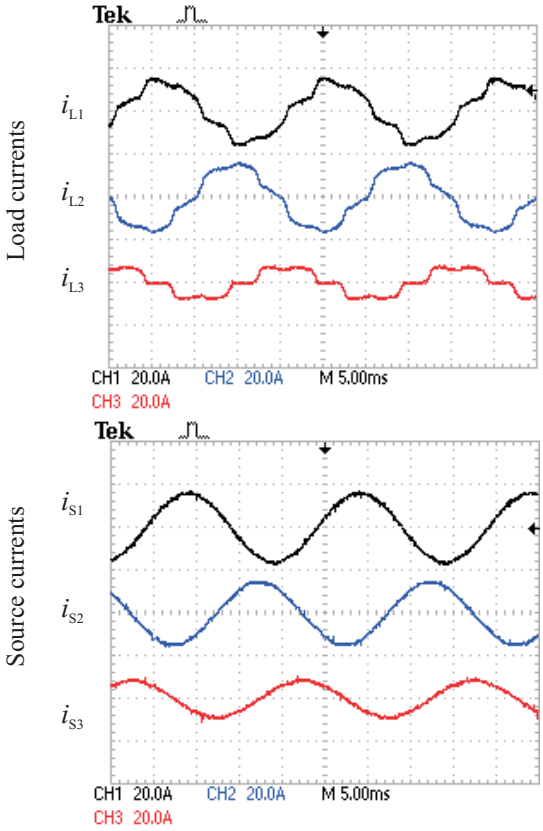


Fig. 15. Experimental results for an unbalanced load – steady state

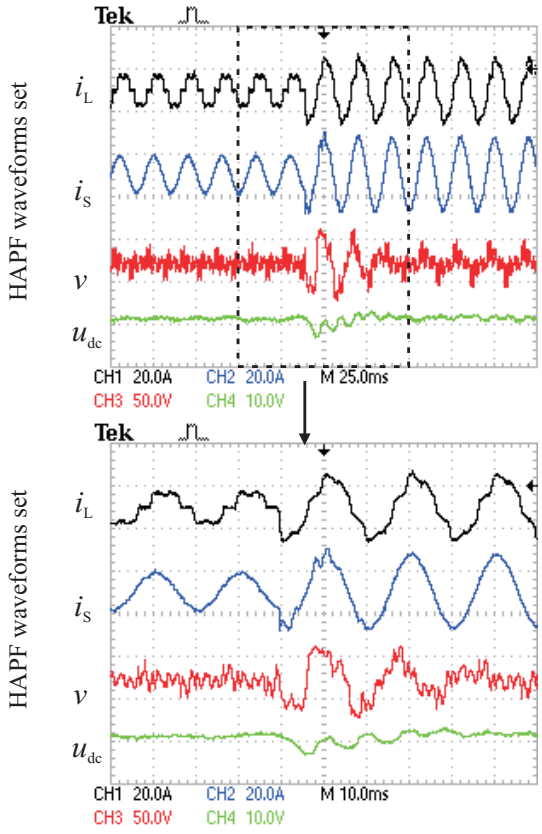


Fig. 16. Experimental results for an unbalanced load – transient state

Table 3
Total harmonic distortion before and after the application of hybrid power filter

| | Balanced load | | | Unbalanced Load | | |
|---|---|---|---|---|---|---|
| | $THDi_{S1}$ | $THDi_{S2}$ | $THDi_{S3}$ | $THDi_{S1}$ | $THDi_{S2}$ | $THDi_{S3}$ |
| Before | 24.8% | 24.6% | 24.7% | 14.0% | 12.4% | 25.3% |
| After | 3.4% | 3.3% | 3.3% | 2.1% | 2.4% | 3.5% |

The presented THD factors certify that the system functioned properly and fulfilled its fundamental purpose, i.e. harmonic filtering. The analysis shows that it allows to increase the gain $K$ more than twice compared to the value used in the tests. However, increasing the gain does not affect the significant improvement of the filtration properties and the need to ensure a sufficiently large margin of stability.

Despite the fact that the instability is a malfunction state and the experimental system is protected from the effects of such conditions, an attempt was made in order to lead to instability. This has been done by artificially increasing the delay in the control system (to 400 $\mu$s – similarly as in simulations). The results for this case are shown in Fig. 17. The 5 kW diode rectifier balanced load was used in this test. Compared to the results shown in Fig. 13, it can be seen that the system did not function properly. Source currents included non-periodic waveforms, therefore there was no point in measuring THD factors. In addition, a problem concerning the DC voltage regulation occurred, which influenced the results as well. However, it has been confirmed by the test that it is possible to bring the analyzed system to an unstable form by increasing the delay time.

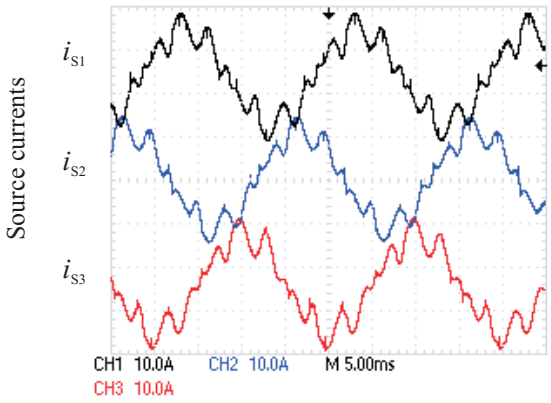


Fig. 17. Experimental results for a balanced load – unstable state (400 $\mu$s delay)

## 8. Conclusions

The stability analysis of a hybrid power filter has been presented in the paper. The analysis shows that it is important to take passive filter parameters into account. The lower capacity allows to use the higher value of hybrid filter gain. Consequently, better filtration properties can be achieved. Another element which influences HAPF stability is the type of a signal filter used in the control algorithm. Using higher order signal filters can cause instability of a system with a hybrid

filter. The analysis also showed the significance of delays in control circuits. Typically, we have no influence on the delay in processing. Nevertheless, an adequate optimization can reduce these delays. This is significant due to the fact that the simulation and experimental results shown in the paper confirmed that delay increasing can lead to incorrect operation of the system – the instability, which could cause a major accident or damage to the system.

The analysis presented in the paper may be used for other types of hybrid filters with closed loop control.

## REFERENCES

[1] J.C. Das, "Passive filters–potentialities and limitations", *IEEE Trans. on Industry Appl.* 40 (1), 232–241 (2004).

[2] H. Akagi, E.H. Watanabe, and M. Aredes, *Instantaneous Power Theory and Applications to Power Conditioning*, Wiley–IEEE Press, London, 2007.

[3] H. Akagi, "Modern active filters and traditional passive filters", *Bull. Pol. Ac.: Tech.* 54 (3), 255–269 (2006).

[4] P. Mattavelli, "A closed-loop selective harmonic compensation for active filters", *IEEE Trans. Ind. Appl.* 37 (1), 81–89 (2001).

[5] T. Płatek, "Power system stability with parallel active filter ensuring compensation of capacitive reactive power of a resonant LC circuit", *Bull. Pol. Ac.: Tech.* 60 (2), 353–361 (2012).

[6] Li Tao and Liu Yongqiang, "The influence of shunt active power filter on stability and performance in considering time-delay", *Mathematical Problems in Engineering* 2013, ID 345748, 9 (2013).

[7] A. Bhattacharya, C. Chakraborty, and S. Bhattacharya, "Parallel-connected shunt hybrid active power filters operating at different switching frequencies for improved performance", *IEEE Trans. Ind. Electronics* 59 (11), 4007–4019 (2012).

[8] P. Salmeroěn and S.P. Litraěn, "A control strategy for hybrid power filter to compensate four-wires three-phase systems", *IEEE Trans. Power Electronics* 25 (7), 1923–1931 (2010).

[9] M. Pasko and D. Buła, "Hybrid active power filters", *Przegląd Elektrotechniczny (Electrical Review)* 83 (7/8), 1–5 (2007).

[10] D. Buła and M. Pasko, "Dynamical properties of hybrid power filter with single tuned passive filter", *Przegląd Elektrotechniczny (Electrical Review)* 87 (1), 91–95 (2011).

[11] W. Tangtheerajaroonwong, T. Hatada, K. Wada, and H. Akagi, "Design and performance of a transformerless shunt hybrid filter integrated into a three–phase diode rectifier", *IEEE Trans. Power Electron.* 22 (5), 1882–1889 (2007).

[12] H. Akagi and K. Isozaki, "A hybrid active filter for a three-phase 12-pulse diode rectifier used as the front end of a medium-voltage motor drive", *IEEE Trans. Power Electronics* 27 (1), 69–77 (2012).

[13] R. Inzunza and H. Akagi, "A 6.6–kV transformerless shunt hybrid active filter for installation on a power distribution system", *IEEE Trans. Power Electron.* 20 (4), 893–900 (2005).

[14] F.Z. Peng, H. Akagi, and A. Nabae, "Compensation characteristics of the combined system of shunt passive and series active filters", *IEEE Trans. Ind. Appl.* 29 (1), 144–152 (1993).

[15] Shi Xiaojie, Shen Yuwen, Zhang Junming, Qian Zhaoming, and F.Z. Peng, "Optimum design consideration and implementation of a parallel hybrid active power filter integrated into a three-phase capacitive diode rectifier", *Proc. APEC 2011* 1, 91–97 (2011).

[16] S. Srianthumrong, H. Fujita, and H. Akagi, "Stability analysis of a series active filter integrated with a double-series diode rectifier", *IEEE Trans. Power Electronics* 17 (1), 117–124 (2002).

[17] Tong Liqing, Qian Zhaoming, Yantao Song, Kuang Naixing, and F.Z. Peng, "Analysis and design of a novel phase-lead compensation control strategy for the SHAPF", *Proc. APEC 2007* 1, 692–697 (2007).

[18] D. Basic, V.S. Ramsden, and P.K. Muttik, "Harmonic filtering of high-power 12-pulse rectifier loads with a selective hybrid filter system", *IEEE Trans. Power Electronics* 48 (6), 1118–1127 (2001).

[19] Wu Longhui, Zhuo Fang, Zhang Pengbo, Li Hui, and Wang Zhaoan, "Stability analysis and controller design of hybrid compensation system with parallel active power filter and parallel capacitors", *Proc. PESC 2007* 1, 1105–1111 (2007).

[20] J. Klamka, A. Czornik, and M. Niezabitowski, "Stability and controllability of switched systems", *Bull. Pol. Ac.: Tech.* 61 (3), 547–554 (2013).

[21] M. Pasko, M. Maciążek, and D. Buła, "Performance and accuracy comparison of fixed and floating-point realizations of the active power filter control algorithm", *Przegląd Elektrotechniczny (Electrical Review)* 85 (1), 162–165 (2009).